Gelation Process of Poly(vinyl alcohol) As Studied by Small-Angle Neutron and Light Scattering

T. Kanaya,* M. Ohkura, H. Takeshita, and K. Kaji

Institute for Chemical Research, Kyoto University, Uji, Kyoto-fu 611, Japan

M. Furusaka

National Laboratory for High Energy Physics, Tsukuba, Ibaraki-ken 305, Japan

H. Yamaoka

Department of Polymer Chemistry, Faculty of Engineering, Kyoto University, Kyoto 606, Japan

G. D. Wignall

Oak Ridge National Laboratory, Oak Ridge, Tennessee 37831

Received October 18, 1994; Revised Manuscript Received February 24, 1995[⊗]

ABSTRACT: We report small-angle neutron scattering (SANS) and light scattering (LS) studies on poly(vinyl alcohol) (PVA) gels formed in a mixture of deuterated dimethyl sulfoxide (DMSO-d_6) and heavy water at 23 °C. It was reported in a previous paper that the SANS intensity $I(Q)$ of the PVA gels is well described by the Ornstein–Zernike (OZ) formula $I(0)/(1 + \xi^2Q^2)$ and Porod's law Q^{-4} for 0.01 Å^{-1} < Q < 0.035 Å^{-1} and 0.05 Å^{-1} < Q < 0.1 Å^{-1}, respectively. In this work, we extended the Q range down to 3×10^{-3} Å^{-1} and found that $I(Q)$ turns up for $Q < 8 \times 10^{-3}$ Å^{-1} to deviate from the OZ formula. This upturn has been assigned to structure due to phase separation based on the results of SANS and LS measurements. In order to investigate the gelation process, time-resolved SANS measurements were carried out on the PVA solutions after quenching to 23 °C from 100 °C. It was found that the correlation length ξ evaluated by the OZ formula in a Q range of 0.01–0.035 Å^{-1} is dominated by concentration fluctuations in the early stage of the gelation before crystallization (t < 200 min) while, after the crystallization initiates, the average correlation distance between the nearest-neighboring crystallites becomes a dominant factor in ξ. Distance distribution function $P(r)$ which is defined by inverse Fourier transformation of the scattering intensity was calculated to see the size and the distribution of the crystallites.

Introduction

Extensive studies on polymer gels have been performed from various points of view[1–4] because a wide variety of polymer gels can provide various interesting features such as responsibilities for electric field, pH, and solvents and high water absorptive power. One of the most interesting gel-forming polymers is poly(vinyl alcohol) (PVA), which can form gels in various kinds of solvents as well as water. Recently, it was reported[5–7] that PVA gels formed from solutions of mixtures of dimethyl sulfoxide (DMSO) and water show very interesting features; e.g., the gels obtained below −20 °C are transparent, the elasticity is very high, and the gelation rate is very fast compared with those from aqueous solutions. These properties depend on the ratio of DMSO to water. In the previous paper,[6] we macroscopically determined the sol–gel diagram and observed the turbidity of the PVA gels in a mixture of DMSO and water (60/40, v/v) as functions of temperature and PVA concentration. It was pointed out that below −20 °C the gelation from the mixture occurs without phase separation, while above −20 °C the phase separation plays a very important role for the gelation.

From microscopic viewpoints, we have also studied PVA gels in mixtures of DMSO-d_6 and heavy water at 23 °C using wide- and small-angle neutron scattering techniques.[8] It was proved that the cross-linking points of the PVA gels are crystallites with sizes of about 70 Å; most crystallites, however, do not work as cross-linking points. It was also clarified that the crystallites are distributed in the concentrated phase after the spinodal decomposition, and the average distance between nearest-neighboring crystallites is about 150–200 Å. Unfortunately, the phase separation was not directly confirmed in the SANS studies although the macroscopic observations strongly suggested that phase separation occurs in the PVA solutions above −20 °C.

In this work, we study the structure of PVA gels in a mixture of DMSO-d_6 and D_2O (60/40, v/v) at 23 °C using a small-angle neutron scattering (SANS) technique. The Q-range in the present SANS measurements has been extended down to 3×10^{-3} Å^{-1} in order to see the structure due to the phase separation as well as the network structure, and time-resolved measurements were also performed on the PVA solutions just after quenching to 23 °C from homogenized solutions at 100 °C to elucidate the formation process of the PVA gels. Furthermore, preliminary light scattering measurements have been made on the PVA solutions in the Q-range of 3.4×10^{-4}–3.6×10^{-3} Å^{-1} to confirm the phase separation. The results of SANS are phenomenologically analyzed without any specific models, and distance distribution functions $P(r)$ which are obtained by inverse Fourier transformation of scattering intensities $I(Q)$ are calculated to see other aspects of the scattering data.

Experimental Section

Materials. Fully saponified atactic poly(vinyl alcohol) (at-PVA) with the number-average degree of polymerization P_n

[⊗] Abstract published in *Advance ACS Abstracts,* April 1, 1995.

0024-9297/95/2228-3168$09.00/0

= 1640 was used for the SANS measurements. The molecular weight distribution, M_w/M_n, is 1.97. The details of the characterization of the PVA sample have been reported elsewhere.[6] The solvent used for SANS was a mixture of deuterated dimethyl sulfoxide (DMSO-d_6) and heavy water (D_2O) with a ratio of 60/40 by volume. Mixtures of DMSO-d_6 and D_2O with various ratios were also employed for the studies of solvent effects.

Gel samples were prepared as follows. A given amount of PVA was dissolved in the solvent at about 130 °C to be homogenized in a sealed glass tube in vacuum in order to avoid contamination from H_2O in atmosphere. Just before the measurements, gel samples were again homogenized at 100 °C for ca. 30 min, and then the solutions were transferred to a quartz sample cell for scattering measurements and quickly quenched to 23 °C within 1 min, and the temperature was controlled to be 23 ± 0.5 °C during the measurements.

Gelation time at 23 °C after quenching from 100 °C was determined macroscopically by a ball-dropping method. The details of the method have been reported elsewhere.[7]

Measurements. SANS measurements were performed with the SANS spectrometer[9] at the National Laboratory for High Energy Physics (KEK), Tsukuba, Japan, and the 30 m SANS spectrometer[10] at the Oak Ridge National Laboratory (ORNL), Oak Ridge, TN. The former is a time-of-flight (TOF) type of small-angle scattering spectrometer and sits at the exit of a neutron guide tube which views a solid methane moderator at 20 K. A converging Soller slit was used before the sample position at 19 m from the moderator so that larger samples (20 mm in width and 30 mm in height) could be used. A two-dimensional area detector was fixed at a position of 3 m from the sample in a vacuum scattering chamber. The Q-range covered with this detector for neutron wavelengths from 3 to 11 Å was 0.01 Å^{-1} < Q < 0.2 Å^{-1}. The sample cell was made of quartz 1 mm thick, and the inner size of the cell was 2 × 20 mm wide and 30 mm high. The observed scattering intensities were corrected for incident neutron spectrum, detector efficiency, sample transmission, and background scattering.

The 30 m SANS spectrometer is installed at the High Flux Isotope Reactor (HFIR) at ORNL. The incident beam of wavelength 4.75 Å ($\Delta\lambda/\lambda$ = 0.06) was collimated by the source (3.5 cm diameter) and sample (1.0 cm diameter) slits separated by a distance of 7.5 m. The area detector (64 × 64 cm^2) with a 1 cm^2 element size, mounted on the rails inside a 20-m vacuum flight path, was positioned at a distance of 19.1 m from the sample to give an effective Q-range of 0.003−0.03 Å^{-1}. The observed scattering intensities were corrected for detector efficiency, sample transmission, and background scattering. The intensities were converted to absolute differential scattering cross sections $d\Sigma/d\Omega$ per unit sample volume (in units of reciprocal centimeters) by means of precalibrated secondary standards.[11] The conversion of the SANS data to an absolute cross section is based on the assumption that the intensity is proportional to the sample thickness and transmission. Thus, samples with different dimensions can be normalized to the same volume to give a coherent cross section, which is an intensive (material) property, independent of the sample dimensions.[12] This result is based on the assumption that neutrons are scattered only once before being detected, and this has been shown to be a reasonable approximation for coherent SANS from polymers[13] and other materials.[14] For incoherent scattering, however, this assumption is not valid, and 1−5-mm samples containing hydrogen (H_2O, H-polymer "blanks", solvent, etc.) give rise to appreciable incoherent−incoherent multiple scattering. Thus the apparent cross section (~1 cm^{-1}) of different hydrogenous (protonated) polymers is a function of the sample thickness.[15] Because such data contain appreciable multiple scattering (which is not proportional to the thickness or transmission), the data cannot be normalized to a true cross section which is independent of the sample dimensions. However, the incoherent background is independent of Q, and empirical methods have been developed to subtract this background to a good approximation.[16,17]

For time-resolved measurements, a short data acquisition time is essential, so that we used cells 5 mm thick for

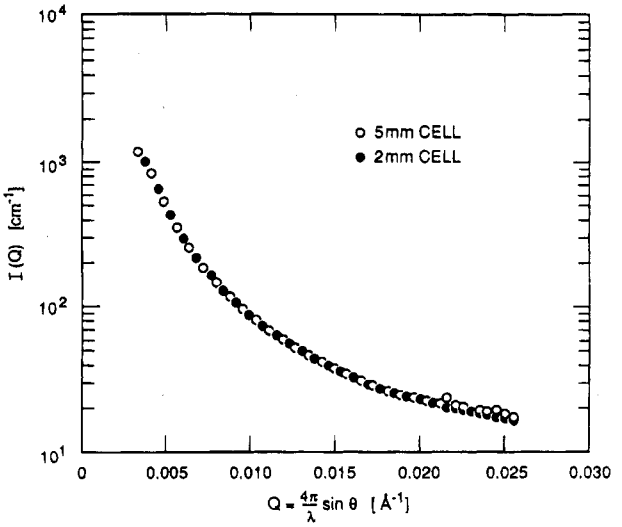

Figure 1. Small-angle neutron scattering intensity $I(Q)$ of PVA gels with C_p = 10 g/dL in DMSO-d_6/D_2O (60/40, v/v) at 23 °C measured with a 30 m SANS spectrometer at ORNL using 2 and 5 mm cells. Multiple scattering effects are negligible under the experimental conditions.

measurements with the 30 m SANS spectrometer. In order to check the effects of multiple scattering, we measured PVA gels with 10 g/dL using 2 and 5 mm thick cells. The neutron transmittances for the these cases were 0.75 and 0.55, respectively, and the latter value is the lowest in the series of the present samples. The scattering cross sections for the two sample thicknesses are shown in Figure 1. Virtually all of the observed intensity arises from coherent single-scattering events, which can be normalized to the same cross section by dividing by the sample thickness and transmission. Thus, 2 mm and 5 mm sample data superimpose exactly over virtually all the Q-range. However, residual effects due to incoherent−incoherent multiple scattering can just begin to be resolved at the highest Q-values as the 5 mm sample has slightly more incoherent−incoherent multiple scattering and hence a slightly higher (flat) background, upon which the main (coherent) signal is superimposed. Corrections for this background were evaluated by measuring the scattering intensity from hydrogenated methanol dissolved in the deuterated mixture of DMSO-d_6 and D_2O in a proportion so that the hydrogen concentration would be the same as that of a given gel sample.

Light scattering measurements were carried out with System 4700 of Malvern Instruments Inc. using an Ar^+ laser (λ = 488 nm, 75 mW) as a light source. The length of scattering vector $Q = 4\pi n \sin\theta/\lambda$, with n being the reflective index, is in a range of 3.6 × 10^{-4}−3.4 × 10^{-3} Å^{-1}. In order to reduce effects of inhomogeneity (speckle) of samples, which arises from the gel structure itself, the measurements were performed by rotating a sample cell (10 mm ϕ).

Results and Discussion

Short Survey of Previous Findings. Before starting the discussion, we will briefly describe the previous findings required to understand the SANS results and our standing point of analyzing the SANS results. In the previous paper,[8] we showed from wide-angle neutron scattering results that there exist crystallites in the PVA gels and the cross-linking points are crystallites. It should be emphasized that not all crystallites in the PVA gels work as cross-linking points, which gives us a basis for interpretation of the SANS results. It was also found that the SANS intensity in the Q-range above 0.01 Å is dominated by the intra- and intercrystallite correlations because crystallite correlations are very strong compared with other correlations such as segment−segment correlations and concentration fluctuations. These facts mean that the SANS

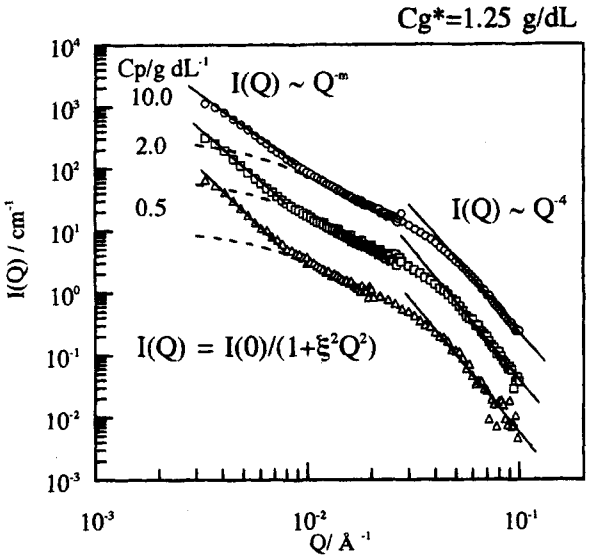

Figure 2. Small-angle neutron scattering intensity $I(Q)$ of PVA gels (C_p = 10 and 2 g/dL) and a sol (C_p = 0.5 g/dL) in DMSO-d_6/D_2O (60/40, v/v) at 23 °C. $I(Q)$'s are well described by $I(Q) \sim Q^{-4}$ for $0.05 < Q < 0.1$ Å^{-1}, $I(Q) = I(0)/(1 + \xi^2Q^2)$ for $0.01 < Q < 0.035$ Å^{-1}, and $I(Q) \sim Q^{-m}$ for $Q < 0.008$ Å^{-1}, which are indicated by solid and dashed lines.

intensity reflects the distribution of the crystallites but not the distribution of the cross-linking points in the system. Many models and theories[18] have been proposed to describe scattering profiles of connected networks or gels. However, it seems too bold to apply such theories to the present PVA gel systems because of the above reason; we therefore analyzed the SANS data without any specific model.

Figure 2 shows the SANS intensities $I(Q)$ of the PVA gels and sols in DMSO-d_6/D_2O (60/40, v/v) for various PVA concentrations, which were kept at 23 °C for 24 h after quenching to 23 °C from 100 °C. $I(Q)$'s above Q = 0.01 Å^{-1} have been reported in the previous paper,[8] where we showed that $I(Q)$ can be well described by the Ornstein–Zernike (OZ) formula and Porod's law:

$$I(Q) = \frac{I(0)}{1 + \xi^2Q^2} \text{ (OZ)} \quad \text{for } 0.01 \text{ Å}^{-1} < Q < 0.035 \text{ Å}^{-1} \quad (1)$$

$$I(Q) \sim Q^{-4} \text{ (Porod)} \quad \text{for } 0.05 \text{ Å}^{-1} < Q < 0.01 \text{ Å}^{-1} \quad (2)$$

where $I(0)$ and ξ are the intensity at $Q = 0$ and a correlation length. The Q-dependences of eqs 1 and 2 are plotted by dashed and solid lines, respectively, in Figure 2 using correlation lengths estimated before.[8] Based on the fact that the cross-linking points are crystallites, the Q^{-4} Porod's law has been therefore attributed to a clear boundary of the crystallites and the correlation length ξ was assigned to the average distance between nearest-neighboring crystallites.[8] The critical gelation concentration C_g* is 1.25 g/dL for P_n = 1640 at 23 °C,[6] so that the sample with C_p = 0.5 g/dL is not macroscopically gel, but sol. As seen from Figure 2, even in $I(Q)$ of the PVA sol with C_p = 0.5 g/dL the Q^{-4} Porod's law is observed, suggesting that microgels are formed in the macroscopic sol and the crystallites in the microgels have also a clear boundary.

Upturn of $I(Q)$ below $Q = 0.008$ Å^{-1}. In the present measurements, we extended the Q-range down to 3×10^{-3} Å^{-1}. As seen in Figure 2, the scattering intensity

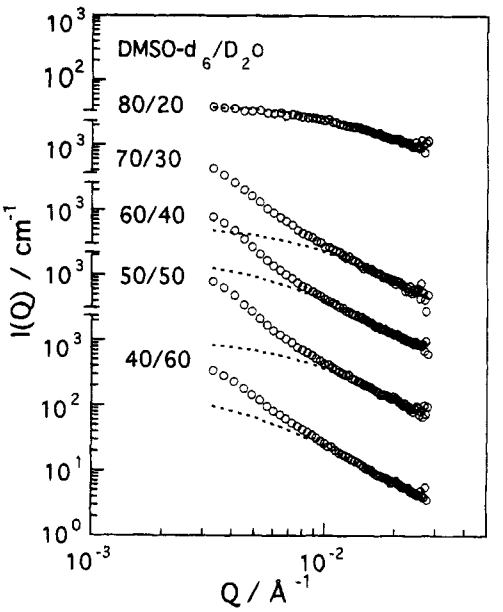

Figure 3. Small-angle neutron scattering intensity $I(Q)$ of PVA gels in DMSO-d_6/D_2O with various ratios. Macroscopically the gel in DMSO-d_6/D_2O (80/20, v/v) is transparent, but others are opaque. Dashed lines represent $I(0)/(1 + \xi^2Q^2)$ with ξ determined by SANS measurements in the Q-range of 0.01–0.1 Å^{-1}.

$I(Q)$ turns up in the Q-range below about 8×10^{-3} Å^{-1} in contradiction to the prediction of $I(0)/[1 + \xi^2Q^2]$ (eq 1). This upturn indicates some inhomogeneity in a spatial scale larger than about 750 Å ($=2\pi/0.008$) in the PVA gels and sols. The problem we have to discuss is what the origin of the inhomogeneity is.

Liquid–liquid phase separation has been strongly expected in the PVA gels at 23 °C from the following macroscopic observations.[6] (1) The gels at 23 °C are opaque, while the gels at low temperatures below about −20 °C are transparent. (2) The critical gelation concentration C_g* is smaller than the chain overlap concentration C* in a temperature range above −20 °C, while it agrees with C* below −20 °C. These facts can be well understood as follows. The gelation process of the PVA is determined by competition between crystallization rate (rate of formation of cross-linking points) and the rate of phase separation or spinodal decomposition. Below −20 °C, the crystallization rate is so fast that the network formation is completed before the phase separation occurs, resulting in transparent gels. On the other hand, above −20 °C the rate of phase separation is comparable to or faster than the crystallization rate so that the phase separation occurs before or during crystallization, producing an infinite network in the concentrated phase to make opaque gels. Concentration of the concentrated phase is thermodynamically determined irrespective of the total polymer concentration. Therefore, the critical gelation concentration C_g* is smaller than the overlap concentration C* above −20 °C.

Based on the above considerations, it would be natural to consider that the upturn of $I(Q)$ below 8×10^{-3} Å^{-1} is due to the phase separation. In order to confirm this idea, SANS measurements have been made on PVA gels in mixtures of DMSO-d_6/D_2O with various ratios. The observed scattering intensities $I(Q)$ in the Q-range of 3×10^{-3}–3×10^{-2} Å^{-1} are shown in Figure 3, where dashed lines represent a function $I(0)/(1 + \xi^2Q^2)$ (eq 1), with ξ estimated by SANS measurements in the Q-range of 0.01–0.1 Å^{-1}. It should be emphasized

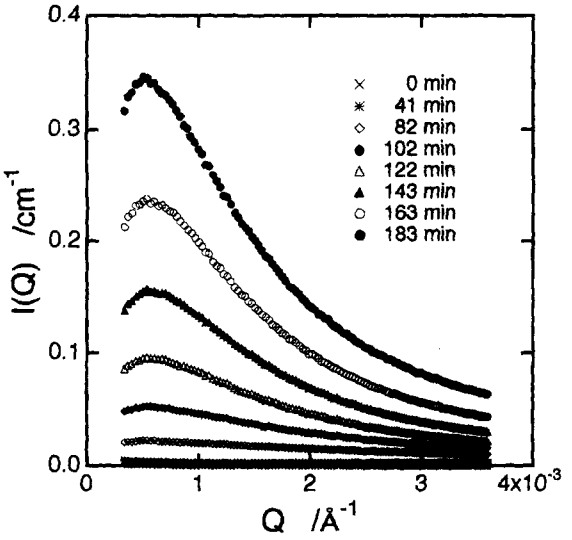

Figure 4. Time evolution of light scattering intensity $I(Q)$ from a PVA solution (C_p = 5 g/dL) in DMSO/H_2O (60/40, v/v) just after quenching to 25 °C from 100 °C. Note that the gelation time determined macroscopically is about 180 min so that all scattering curves are from sols.

that the PVA gel in DMSO-d_6/D_2O (80/20) is transparent, while all other gels are opaque, suggesting that phase separation does not occur only in the case of DMSO-d_6/D_2O (80/20, v/v). Corresponding to this macroscopic observation, only $I(Q)$ from the PVA gel in DMSO-d_6/D_2O (80/20, v/v) does not show the upturn in the low Q-range below 0.01 Å^{-1}. On the other hand, $I(Q)$'s of the opaque PVA gels in the other solvents show a clear upturn in the low Q-range below ca. 0.01 Å^{-1}, suggesting that the upturn is due to the liquid–liquid phase separation.

In order to get more evidences for the phase separation, time-resolved light scattering (LS) measurements on a PVA solution in DMSO/H_2O (60/40, v/v) have been carried out in the Q-range of 3.4×10^{-4}–3.6×10^{-3} Å^{-1} after quenching to 25 °C from 100 °C. The high Q-range of LS is overlapped with the low Q-range of SANS. Figure 4 shows the observed time evolution of $I(Q)$ up to 183 min after quenching. The gelation time for P_n = 1640 at 23 °C was macroscopically determined to be about 180 min, meaning that all the scattering curves come from sols, but not from gels. The scattering intensity $I(Q)$ shows a maximum at about $Q = 0.5 \times 10^{-3}$ Å^{-1} and the maximum position Q_m does not change during the measurements, while the maximum intensity I_m increases according to an exponential law in the early stage shorter than ca. 100 min. These facts agree with the predictions for the early stage of spinodal decomposition,[19,20] confirming again that the phase separation or spinodal decomposition certainly occurs in the DMSO/H_2O (60/40, v/v) solution of PVA during the gelation process. A more detailed analysis of the light scattering data is beyond the aim of this paper, and it will be reported elsewhere. Here, we concentrate on the results of SANS. In any case, we can conclude that the upturn in the neutron scattering intensity below $Q = 8 \times 10^{-3}$ Å^{-1} is assigned to the structure due to the phase separation.

Following the above discussion in addition to the previous results,[8] the scattering intensity $I(Q)$ of the PVA gels can be approximately classified into three regions, termed regions I–III, the Q-ranges of which are Q < 0.008 Å^{-1}, 0.01 Å^{-1} < Q < 0.035 Å^{-1}, and 0.05 Å^{-1} < Q < 0.1 Å^{-1}, respectively. Thus,

$$I(Q) = \begin{cases} I_1(Q) & \text{for } Q < 0.008 \text{ Å}^{-1} \\ I_2(Q) & \text{for } 0.01 < Q < 0.035 \text{ Å}^{-1} \\ I_3(Q) & \text{for } 0.05 < Q < 0.1 \text{ Å}^{-1} \end{cases} \quad (3)$$

These three components $I_1(Q)$, $I_2(Q)$, and $I_3(Q)$ are considered to come dominantly from the structure of the phase separation, the correlations between neighboring crystallites, and the surface structure of the crystallites, respectively. The boundaries between the regions are more clearly recognized in the plot of $Q^2I(Q)$ vs Q in double-logarithmic form (see Figure 6). As shown before, the latter two contributions $I_2(Q)$ and $I_3(Q)$ are described by eqs 1 and 2, respectively. The first contribution $I_1(Q)$ seems to follow a power law (see Figure 2).

$$I_1(Q) \sim Q^{-m} \quad (4)$$

The exponents m are 3.6, 3.2, 3.2, and 2.5 for C_p = 0.5, 2.0, 5.0, and 10.0 g/dL, respectively. One possible interpretation for the power law is that $I_1(Q)$ is dominated by the boundary structure due to the phase separation. We showed that the spinodal decomposition takes place in the PVA gels at 23 °C, leading to a two-phase structure composed of concentrated and diluted phases. The boundary structure should be observed in some Q-range above the peak position Q^m of the light scattering profile $I(Q)$. In the case of polymer blends, boundary structure due to phase separation was clearly observed.[21] Provided we are seeing the boundary structure between the two phases in the Q-range below 0.008 Å^{-1}, we may apply the surface fractal concept to $I_1(Q)$. According to the concept of surface fractal,[22] the exponent m is related to the surface fractal dimension d_s through $m = 2d - d_s$ in d-dimensional space. In three-dimensional space, for example, the range of d_s is from 2 to 3, corresponding to the range of m from 4 to 3. If the boundary is clear, Porod's law [$I(Q) \sim Q^{-4}$] would be observed. For the present PVA gels, all values of m are less than 4, suggesting that the boundary is not very clear (m = 3.6, 3.2, and 3.2 for C_p = 0.5, 2.0, and 5.0 g/dL), or it would not be impossible to be regarded as a boundary (m = 2.5 for C_p = 10 g/dL). The exponent m decreases with increasing the PVA concentration. This can be qualitatively understood as follows. Phase separation of the PVA gels at 23 °C occurs in competition with gelation or network formation. With an increase in the PVA concentration C_p, the gelation rate or crystallization rate increases, resulting that the structural formation due to the phase separation is prevented by the production of the network structure, and so it is not completed. Therefore, the boundaries between the concentrated and dilute phases are not clear, especially for the PVA gels with high concentrations.

Time-Resolved SANS Measurements. Time-resolved measurements of SANS have been carried out on a solution of PVA (C_p = 3.5, 5, and 10 g/dL) in DMSO-d_6/D_2O (60/40, v/v) just after quenching to 23 °C from 100 °C. Time evolution of the scattering intensity $I(Q)$ for C_p = 5 g/dL is shown in Figure 5 in a double-logarithmic form of $I(Q)$ vs Q. As seen in Figure 5, $I(Q)$ increases with time up to about 600 min, but no changes are observed in $I(Q)$ after that time. This suggests that the gelation is completed by this time and the produced gel is in a quasi-equilibrium state, at least, in the Q-range examined. Note that very slow changes of the PVA gels such as volume change are observed during

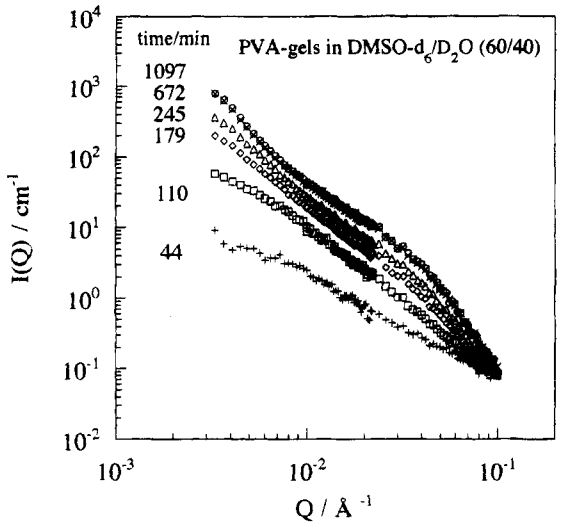

Figure 5. Time evolution of small-angle neutron scattering intensity $I(Q)$ of PVA sols and gels (C_p = 5 g/dL) in DMSO-d_6/D_2O (60/40, v/v) just after quenching from to 23 °C from 100 °C. t = 44 min (+), 110 (□), 179 (◇), 245 (△), 672 (×) and 1097 (○). The gelation time is about 180 min. Plot of $I(Q)$ vs Q in double-logarithmic form.

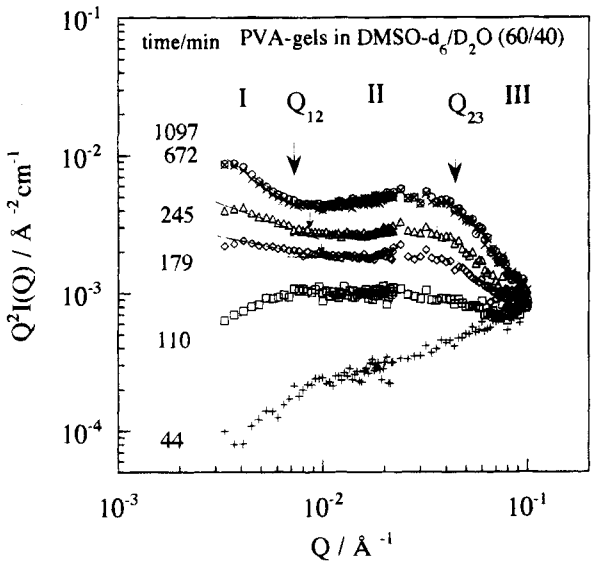

Figure 6. Same as for Figure 5. Plot of $Q^2I(Q)$ vs Q in double-logarithmic form.

several weeks to several months after attaining quasi-equilibrium. However, in the time scale of the present experiments, the slow changes are negligible. Before discussing the results of time-resolved SANS each Q-range where the three distinct scattering regions described above appear needs to be made clear. The boundaries of these regions will become clearer when it is plotted in a $Q^2I(Q)$ vs Q fashion. Figure 6 shows such a plot; the boundaries between regions I and II and regions II and III are indicated by Q_{12} and Q_{23}, respectively.

First, we will discuss the time evolution of scattering intensity due to the phase separation, $I_1(Q)$. For the time region t > 180 min, the upturn originating from the phase-separation structure is observed; the rising-up point corresponds to the boundary Q_{12} between regions I and II as indicated by downward arrows in Figure 6. The value of Q_{12} for t > 180 min shifts to smaller Q with time, suggesting that the structure due to phase separation develops in size and amplitude. It

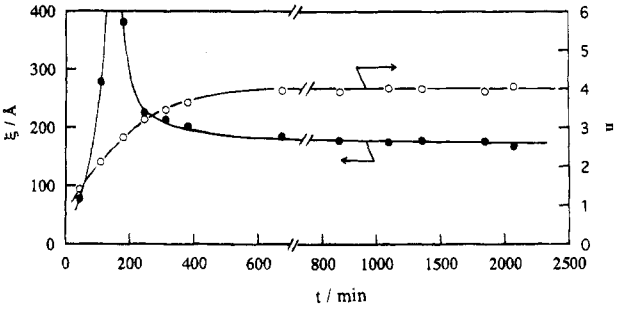

Figure 7. Time evolution of the correlation length ξ (●) and the exponent n (○) for PVA sols and gels (C_p = 5 g/dL) in DMSO-d_6/D_2O (60/40 v/v) just after quenching to 23 °C from 100 °C.

should be noted that the gelation time determined macroscopically for this system is about 180 min. This means that the phase separation proceeds even after macroscopic gelation. Macroscopic gelation is considered as that, at least, one infinite cluster is formed in the system, while all polymer chains are not necessarily incorporated into the infinite cluster. Since the remaining finite clusters as well as unincorporated single polymer chains can diffuse in the system, the phase separation proceeds even after the macroscopic gelation. This picture agrees with the fact that the turbidity of the gel continues to increase after gelation (see Figure 4 in ref 6). For t < 180 min before gelation, the upturn is not recognized, but the effect of the phase separation on $I(Q)$ is not negligible in region I because light scattering intensity $I(Q)$ in this time region shows a clear maximum originated from the phase-separation structure (see Figure 4).

As seen in Figure 6, the time evolution of $I(Q)$ in region I is clearly different from that in region II; the growth rate of $I(Q)$ in region I is larger than that in region II, suggesting that the $I(Q)$ of region II is dominated by some fluctuations other than phase separation.

For t > 600 min after gelation, the scattering intensities $I(Q)$ in regions II and III are governed by intra- and intercrystallite correlations and are well described by eqs 1 and 2, respectively, as shown before. Here, the scattering intensities $I(Q)$'s for t < 600 min were also analyzed in the same way as for t > 600 min; i.e., $I(Q)$'s in the Q-range of 0.01−0.035 Å^{-1} were fitted with $I(0)/[1 + \xi^2Q^2]$ (eq 1) to evaluate the correlation length ξ, and $I(Q)$'s in the Q-range of 0.05−0.1 Å^{-1} were assumed to be described by a power law Q^{-n} to evaluate the exponent n. For t > 600 min, $I(Q)$'s in regions II and III provide information on the distribution of the crystallites and the size of the crystallites, respectively. However, $I(Q)$'s for t < 600 min are no longer determined only by the crystallites because the structure of the crystallites may be loose or not completely constructed. Therefore, it should be kept in mind that the correlation length ξ and the exponent n for t < 600 min are apparent values.

Time evolutions of the evaluated correlation length ξ and the exponent n are shown in Figure 7 for a solution of PVA (C_p = 5 g/dL) in DMSO-d_6/D_2O (60/40, v/v). The correlation length ξ increases rapidly with time in the early stage of gelation, and after diverging or having a maximum at t = 150 min, it decreases to about 180 Å. The leveling-off value of ξ can be attributed to the average distance between the nearest-neighboring crystallites as discussed before. In the early stage, however, the crystallites may not be well constructed so that it

would be impossible to attribute it to the intercrystallite correlations. What governs the correlation length ξ before gelation? It would be impossible to attribute this to the phase-separation structure because the value of ξ is too small to be related to the phase separation, the characteristic length of which is about 12 000 Å ($=2\pi/Q_m$; see Figure 4). Furthermore, according to the theory,[19,20] the characteristic length of spinodal decomposition should be independent of time in the early stage; in contrast, ξ actually increases with time for t < 150 min. Recently, we have found that density fluctuations occur during the induction period of crystallization of a poly(ethylene terephthalate) glass[23,24] and the kinetics is very similar to that of spinodal decomposition. Taking into account that crystallite correlations are dominant in region II after gelation t > 200 min, we assign the correlation length ξ to a characteristic length of the concentration fluctuations during the induction period of crystallization of PVA.

The exponent n in region III is 4 for t > 600 min, suggesting that the crystallites have clear boundaries. Before gelation, however, the exponent n is less than 4. We could apply the surface fractal concept to the growth of n, at least, in the range of n near 4. The growth of n for t < 600 min may correspond to a process in which the surface of the crystallites becomes clear with time. According to the concept of surface fractal,[22] the range of n should be from 4 to 3, corresponding to a change from two dimension to three dimension. The exponent n exceeds 3 at around t = 200 min, which may correspond to the time when the boundaries of the crystallites could be defined. This idea is also supported by the fact that the correlation length ξ is dominated by the correlation between the crystallites after about 200 min. For 200 min < t < 600 min, the crystallites are therefore considered to have rough surfaces. In the early stage before gelation for t < 180 min, the exponent n is less than 3, suggesting that the exponent is no longer related to the boundaries of the crystallites. It may be because the crystallites are not well constructed and the boundary cannot be defined. It is therefore considered that $I(Q)$ in region III for t < 200 min is governed by concentration fluctuations during the induction period of crystallization as well as in region II. In fact, $I(Q)$'s in both regions II and III at t = 44 and 110 min are approximately described by a single power law.

In order to see other aspects of the time evolution of SANS, especially the size and distribution of the crystallites, distance distribution functions $P(r)$ were calculated by inverse Fourier transformation of $I(Q)$.[8,25]

$$P(r) \sim (2/\pi)\int rQI(Q)\sin(rQ)\,dQ \qquad (5)$$

$$\sim 4\pi r^2\gamma(r)$$

where $\gamma(r)$ is a pair correlation function. In this calculation, we have to extrapolate $I(Q)$ in the lower and higher Q regions. In order to get information on the size and distribution of the crystallites, we can eliminate the effects of the phase-separation structure on $P(r)$. For this purpose, the extrapolation was made by employing two functions of $I(0)/[1 + \xi^2Q^2]$ and aQ^{-n} for the lower and higher Q-ranges, respectively, in the same way as before.[8] The parameters ($I(0)$ and ξ, and a and $-n$) were determined by fitting $I(0)/[1 + \xi^2Q^2]$ and aQ^{-n} to the observed $I(Q)$ in the Q ranges of 0.01 < Q < 0.035 Å^{-1} and 0.05 < Q < 0.1 Å^{-1}, respectively. This procedure did neglect deviation of $I(Q)$ from $I(0)/[1 + \xi^2Q^2]$ in the Q-range below 0.01 Å^{-1}, especially the upturn in $I(Q)$ below 8×10^{-3} Å^{-1} for t > 600 min, meaning that we have eliminated the structure due to the phase separation in $P(r)$. Time evolution of $P(r)$ is shown in Figure 8 for a solution of PVA (C_p = 5 g/dL) in DMSO-d_6/D_2O (60/40, v/v) after quenching to 23 °C. Intensity of $P(r)$ increases with time up to about 600 min, corresponding to the time evolution of $I(Q)$. An outstanding feature in $P(r)$ is that a long-range correlation different from the crystallite correlations for t > 200 min is observed at t = 110 and 179 min, which can be assigned to concentration fluctuations during the induction period of crystallization. When time exceeds 200 min, correlation in the r range of about 70−250 Å increases according to the growth of the crystallites. As demonstrated in the previous paper,[8] the $P(r)$'s in the r ranges below and above ca. 150 Å are mainly dominated by the intra- and intercrystallite correlations, respectively. In order to separate the two contributions, we fitted the observed $P(r)$ in the small r range with a model function for the intracrystallite correlation. This model function was calculated under the assumption that the shape of the crystallites is a sphere and the size (radius) distribution of the crystallites can be represented by a Gaussian. Fitting was made on $P(r)$ at t = 245, 380, and 2070 min because $P(r)$ for t < 200 min is not dominated by the intra- and intercrystallite correlations. The dotted lines in Figure 9 show the results of the fits, which corresponds to a distance distribution function due to the intracrystallite correlations $P_{intra}(r)$. The sizes (radii) and the size distributions (root of the dispersion σ_c) are listed in Table 1. The intercrystallite correlation $P_{inter}(r)$ is given by dashed lines in Figure 9, which was obtained by subtracting $P_{intra}(r)$ from the total $P(r)$. The peak position of $P_{inter}(r)$ does not change with time, suggesting that the average distance between the neighboring crystallites is almost independent of time for t > 200 min. On the other hand, the size of the crystallites slightly increases with time, corresponding to growth of the crystallites.

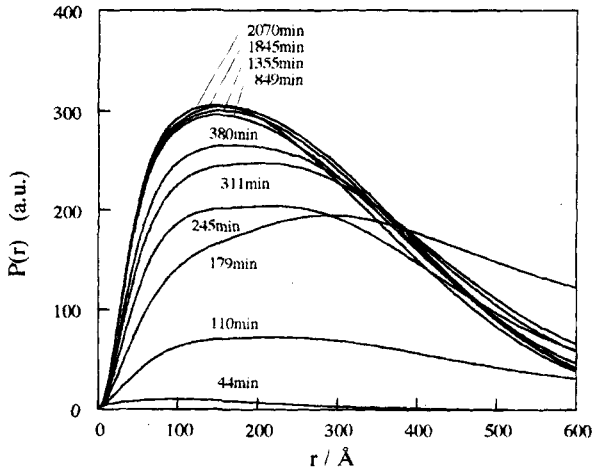

Figure 8. Time evolution of distance distribution function $P(r)$ of PVA sols and gels (C_p = 5 g/dL) in DMSO-d_6/D_2O (60/40, v/v) just after quenching to 23 °C from 100 °C. The gelation time is about 180 min.

Conclusions

The PVA gels in DMSO-d_6/D_2O (60/40, v/v) have been investigated by small-angle neutron scattering technique in a Q-range of 3×10^{-3}−0.1 Å^{-1}. In this study, it was found that SANS intensity $I(Q)$ from the PVA

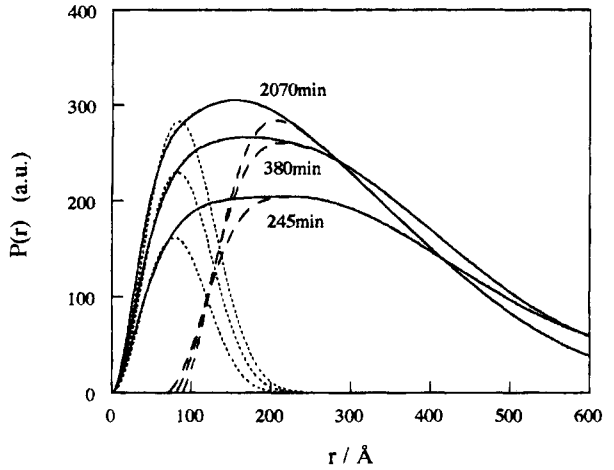

Figure 9. Distance distribution functions for intra- and intercrystallite correlations $P_{intra}(r)$ (dotted lines) and $P_{inter}(r)$ (dashed lines) for PVA gels in DMSO-d_6/D_2O (60/40, v/v) at t = 245, 380, and 2070 min after quenching to 23 °C. The intracrystallite correlation $P_{intra}(r)$ was obtained by fitting a model function with observed $P(r)$ (solid lines) in the small r range. The model function was calculated under the assumption that the shape of the crystallite is a sphere and the distribution of the sizes can be represented by a Gaussian. The intercrystallite correlation $P_{inter}(r)$ was obtained by subtracting $P_{intra}(r)$ from the total $P(r)$.

Table 1. Radius of the Crystallite R and the Distribution of the Radius σ_c Evaluated by the Fitting of $P(r)$

time/min	R/Å	σ_c/Å
245	73.9	16.0
380	76.6	17.8
2070	77.6	19.2

gels shows a clear upturn in the Q-range below 8×10^{-3} Å^{-1}, which has been assigned to the structure due to the phase separation based on the results of solvent effects on SANS and preliminary light scattering measurements as well as previous macroscopic observations. Time-resolved SANS measurements suggested that in the early stage of the gelation the scattering intensity $I(Q)$ in the Q-range above 0.01 Å^{-1} is dominated by concentration fluctuations during the induction period of crystallization and is gradually governed by the inter- and intracrystallite correlations according to the developments of the crystallites. On the other hand, time evolution of $I(Q)$ below 0.01 Å^{-1} is dominated by the development of the phase-separation structure. Further analysis of the light scattering results will be reported for characterization of the structure due to the phase separation in the future.

Acknowledgment. This work was supported in part by a Japan–U.S. Neutron Scattering Collaboration Program supported by the Ministry of Education, Science and Culture, Japan, and also by the Division of Materials Sciences, U.S. Department of Energy, under Contract No. DE-AC05-840R21400 with Martin Marietta Energy Systems Inc.

References and Notes

(1) *Biological and Synthetic Polymer Networks*; Kramer, O., Ed.; Elsevier Applied Science: London, 1988.
(2) *Physical Networks: Polymers and Gels*; Buchard, W., Ross-Murphy, S. B., Eds.; Elsevier Applied Science: London, 1990.
(3) Guenet, J. *Thermoreversible gelation of polymers and biopolymers*; Academic Press: London, 1992.
(4) *Synthesis, Characterization, and Theory of Polymeric Networks and Gels*; Aharoni, S. M., Ed.; Plenum: New York, 1992.
(5) Hyon, S.; Cha, W.; Ikada, Y. *Polym. Bull.* **1989**, *22*, 119.
(6) Ohkura, M.; Kanaya, T.; Kaji, K. *Polymer* **1992**, *33*, 3689.
(7) Ohkura, M.; Kanaya, T.; Kaji, K. *Polymer* **1992**, *33*, 5044.
(8) Kanaya, T.; Ohkura, M.; Kaji, K.; Furusaka, M.; Misawa, M. *Macromolecules* **1994**, *27*, 5069. Kanaya, T.; Ohkura, M.; Kaji, K.; Furusaka, M.; Misawa, M.; Yamaoka, H.; Wignall, G. D. *Physica* **1992**, *B180/181*, 549.
(9) Ishikawa, Y.; Furusaka, M.; Niimura, N.; Arai, M.; Hasegawa, K. *J. Appl. Crystallogr.* **1986**, *19*, 229.
(10) Koehler, W. C. *Physica B* **1986**, *137*, 320.
(11) Wignall, G. D.; Bates, F. S. *J. Appl. Crystallogr.* **1987**, *20*, 28.
(12) Wignall, G. D. In *The Physical Properties of Polymers*; Mark, J. E., Ed.; ACS Books: Washington, DC, 1993; p 313.
(13) Goyal, P. S.; King, J. S.; Summerfield, G. C. *Polymer* **1983**, *24*, 131.
(14) Schelten, J.; Schmatz, W. *J. Appl. Crystallogr.* **1980**, *13*, 385.
(15) O'Reilly, J. M.; Teegarden, D. M.; Wignall, G. D. *Macromolecules* **1985**, *18*, 2747.
(16) Hayashi, H.; Flory, P. J.; Wignall, G. D. *Macromolecules* **1983**, *16*, 1328.
(17) Dubner, W. S.; Schultz, J. M.; Wignall, G. D. *J. Appl. Crystallogr.* **1990**, *23*, 469.
(18) Zemb, T. In *Neutron, X-Ray and Light Scattering: Introduction to an Investigative Tool for Colloidal and Polymeric Systems*; Linder, P., Zemb, T., Eds.; North-Holland: Amsterdam, The Netherlands, 1991; p 117.
(19) Cahn, J. W.; Hilliard, J. E. *J. Chem. Phys.* **1958**, *28*, 258.
(20) Cahn, J. W. *J. Chem. Phys.* **1965**, *42*, 93.
(21) Jinnai, H.; Hasegawa, H.; Hashimoto, T.; Han, C. C. *Macromolecules* **1991**, *24*, 282.
(22) Martin, J. E.; Hurd, A. J. *J. Appl. Crystallogr.* **1987**, *20*, 61.
(23) Imai, M.; Mori, K.; Mizukami, T.; Kaji, K.; Kanaya, T. *Polymer* **1992**, *33*, 4451.
(24) Imai, M.; Mori, K.; Mizukami, T.; Kaji, K.; Kanaya, T. *Polymer* **1992**, *33*, 4457.
(25) Kaji, K.; Urakawa, H.; Kanaya, T.; Kitamaru, R. *Macromolecules* **1984**, *17*, 1835.

MA9461310